Field test and load spectrum compilation on the drive shaft of feeding and conveying device for combine harvesters

Fu Zhang[1*], Xiaoshuai Li[1,2], Shengcao Huang[3], Zhiqiang Guo[3], Zhiwei Yu[2], Huawei He[2], Pengfei Wang[4]

(1. *College of Agricultural Equipment Engineering, Henan University of Science and Technology, Luoyang 471003, Henan, China*; 2. *National Innovation Agricultural Equipment Quality Test Technology (Luoyang) Co., Ltd., Luoyang 471000, Henan, China*; 3. *National Institute of Agri-machinery Innovation & Creation, Luoyang Smart Agricultural Equipment Institute Co., Ltd., Luoyang 471000, Henan, China*; 4. *College of Mechanical and Electrical Engineering, Agricultural University of Hebei, Baoding 071001, Hebei, China*)

Abstract: The feeding and conveying device for combine harvester is often prone to blockage during field harvesting operations, which is why it is very important to study the working load of its drive shaft. To obtain the true load of the drive shaft of the feeding and conveying device for combine harvester under typical field operating conditions, the domestic 12 kg/s wheeled combine harvester was taken as the test object and a field load test system was constructed based on the perception of strain torque sensor and speed sensor. Through the field load tests, the results showed that the maximum power consumption of the drive shaft was 4.06 kW under the harvesting operation conditions and the average power consumption was 1.56 kW. Based on the rainflow counting method, the two-dimensional extrapolation load spectrum of the key power input section of the drive shaft under typical operating conditions was compiled by using the matrix cyclic period extrapolation method, which can provide loading conditions for the fatigue life test of the drive shaft of the feeding and conveying device for combine harvester. This method will provide a basis for the power matching of the working device of the harvester and a reference for the anti-fatigue design of the transmission system of the combine harvester.

Keywords: combine harvester, feeding and conveying device for combine harvester, load test system, rainflow counting method, matrix cyclic period extrapolation method

DOI: 10.25165/j.ijabe.20261902.10258

Citation: Zhang F, Li X S, Huang S C, Guo Z Q, Yu Z W, He H W, et al. Field test and load spectrum compilation on the drive shaft of feeding and conveying device for combine harvesters. Int J Agric & Biol Eng, 2026; 19(2): 152–157.

1 Introduction

The feeding and conveying device for combine harvester, as the core component connecting the header to the threshing unit, is crucial for the efficient operation of the entire machine, ensuring continuous and stable material flow[1-3]. To ensure efficient and stable conveying during the operation season, it is particularly crucial to obtain the field load of the drive shaft of the feeding and conveying device for combine harvester and verify the power performance and reliability of the transmission system[4].

The field load test of the drive shaft of the feeding and conveying device for combine harvester requires collecting the changes in torque and rotational speed, evaluating the working load conditions, and obtaining the bench test load spectrum after editing and processing. Bench fatigue tests using load spectra can significantly shorten the fatigue life verification cycle and have been widely applied in the automotive and aviation fields, but less in agricultural machinery. For the actual load collection under operating conditions of non-road machinery such as agricultural machinery and construction machinery, scholars at home and abroad have developed load testing systems based on strain torque sensors and speed sensors to reflect the load characteristics of mechanical components[5-10]. In terms of the compilation and application of load spectra, scholars have commonly used time-domain extrapolation or rainflow basin extrapolation methods for load data to obtain load spectra that can be used for bench tests and to predict their fatigue life[11-17].

Currently, limited research has been conducted on field load spectrum testing for agricultural machinery, particularly regarding load spectrum measurements of key shafting components in combine harvesters. Meanwhile, a mature methodology for load spectrum compilation and extrapolation tailored to field operating conditions of agricultural machinery has not yet been established.

Based on actual production requirements, combined with the load conditions of the drive shaft of the feeding and conveying device for combine harvester under actual operating conditions, using a large domestic double longitudinal axial flow combine harvester as the test model, the drive shaft of the feeding and conveying device for combine harvester was selected as the research object, a field load test system under typical operating conditions was established, load data was obtained, and the load

Received date: 2025-11-11 **Accepted date:** 2026-03-13

Biographies: Xiaoshuai Li, MS candidate, Engineer, research interest: agricultural machinery test and inspection, Email: 339564965@qq.com; **Shengcao Huang**, PhD candidate, Senior Engineer, research interest: agricultural machinery test and inspection, Email: huangshengcao@chiaic.com; **Zhiqiang Guo**, PhD candidate, Engineer, research interest: agricultural machinery test and inspection, Email: guozhiqiang@chiaic.com; **Zhiwei Yu**, MS, Engineer, research interest: agricultural machinery test and inspection, Email: yuzhiwei@chiaic.com; **Huawei He**, Engineer, research interest: agricultural machinery test and inspection, Email: hehuawei@chiaic.com; **Pengfei Wang**, MS, Associate Professor, research interest: intelligent agricultural equipment, Email: wpf5769@126.com.

***Corresponding author: Fu Zhang**, PhD, Professor, Assistant Dean, research interest: agricultural informatization and intelligent agricultural equipment. College of Agricultural Equipment Engineering, Henan University of Science and Technology, Luoyang 471003, Henan, China. Tel: +86-13592065683, Email: zhangfu30@126.com.

spectrum for bench tests was compiled using the rainflow-domain extrapolation method, which can provide a basis for the reliability verification of the working device of the combine harvester.

2 The structure and working principle of the feeding and conveying device for combine harvester

The main function of the feeding and conveying device for combine harvester is to transport the harvested crops from the header to the threshing device, as shown in Figure 1. The structure mainly consists of the box body, conveyor chain, chain rake, etc. After the header cuts the grain, the grain will be sent into the conveyor trough through the threshing wheel and the conveyor chain. The drive and driven wheels on the conveyor device transmit power to the conveyor trough via chains or belts. Scrapers on the chain convey the crop to the threshing mechanism. The conveyor trough ensures smooth crop flow by adjusting the speed of the conveyor chain. Rubber pads and curved anti-spill plates are installed between the trough's discharge outlet and the thresher's inlet to prevent grain leakage[18-20].

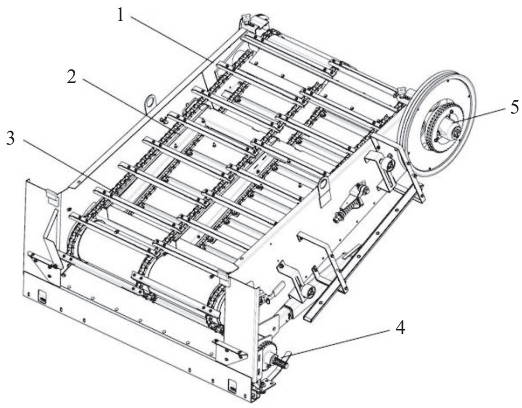

1. Box body 2. Conveyor chain 3. Chain rake 4. Driven shaft of feeding and conveying device for combine harvester 5. Drive shaft of feeding and conveying device for combine harvester

Figure 1 Structural diagram of feeding and conveying device for combine harvester

3 Setup of the field load test system

3.1 Overall scheme design

The strain torque measurement principle was employed to construct the field load test system for acquiring torque signals at the power input end of the drive shaft. Hall sensors were used to obtain the rotational speed signal. Shaft-end slip rings were used to transmit data signals. The system architecture, shown in Figure 2, primarily consists of the torque acquisition module, the Revolutions Per Minute (RPM) acquisition module, the signal transmission device, the signal pickup device, the computer, and the data analysis software. Parameters of sensors and related hardware are listed in Table 1.

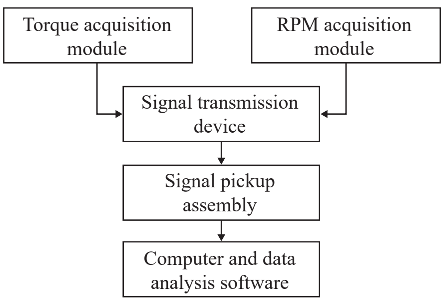

Figure 2 Load test system architecture

Table 1 Sensors and related hardware parameters

Test hardware	Model	Parameters
Strain gauge	BE350-3HA(11)-Q30	350 Ω Sensitivity coefficient 2.1
Slip ring	HT035018-018	Dynamic resistance ≤10 mΩ
Signal acquisition device	SoMat eDAQ	32-ch EBRG, 100 kHz/ch

3.2 Test system setup

3.2.1 Calibration and installation of torque sensors

After rough grinding, fine grinding, cleaning, and drying, strain gauges were bonded to the drive shaft surface at a position 200 mm inward from the input-end bearing of the transmission shaft. The gauges were arranged in a 45°/135° grid angle configuration to form a full Wheatstone bridge circuit with 350 Ω resistance. Following installation, insulation was applied to the strain gauges and connecting wires. Next, 704 silicone adhesive was evenly applied to the strain gauges, leads, terminals, and wires. Finally, the assembly was uniformly wrapped with electrical tape for sealing.

Static calibration was required to verify the characteristics such as repeatability, stability, and linearity of the torque sensor on the drive shaft of the feeding and conveying device for combine harvester. The corresponding bearing housing, fixed turntable, and calibration bracket are designed according to the diameter of the drive shaft of the feeding and conveying device for combine harvester and the bearing installation position to form the calibration test bench, as shown in Figure 3.

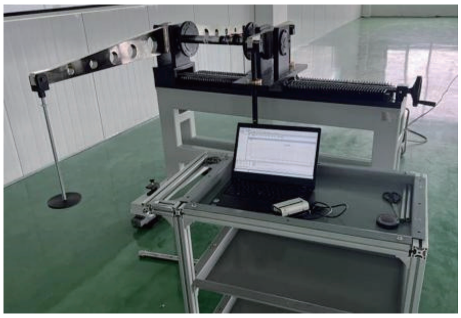

Figure 3 Torque sensor calibration test bench

During the calibration, the drive shaft equipped with the torque sensor was loaded six times, and the calibration data were recorded. Repeated calibration was performed every other day to verify the stability of the torque sensor. Based on the calibration data, the linear regression equation can be used to obtain the proportional coefficient, that is:

$$b=\frac{\sum_{i=1}^{n}\left(X_i-\bar{X}\right)\left(Y_i-\bar{Y}\right)}{\sum_{i=1}^{n}\left(X_i-\bar{X}\right)^2} \tag{1}$$

where, X_i is the measured value of the input quantity at a certain point, N·m; $\bar{X}$ is the arithmetic mean of the measured input; Y_i is the value of the measured output at a certain point, $\mu\varepsilon$; $\bar{Y}$ is the arithmetic mean of the measured output at a certain point; n is the measured number of points; b is the value of the proportional coefficient, $\mu\varepsilon$/N·m.

After calculation, the calibration ratio coefficient b is determined to be 1.443. The calibration data of external force and strain were linearly fitted as shown in Figure 4, and the calibration curve equation was obtained as Y=1.443X–5.8199, R^2=0.9969. The error between the load values calculated by the calibration function and the experimentally calibrated load values is all within 1%.

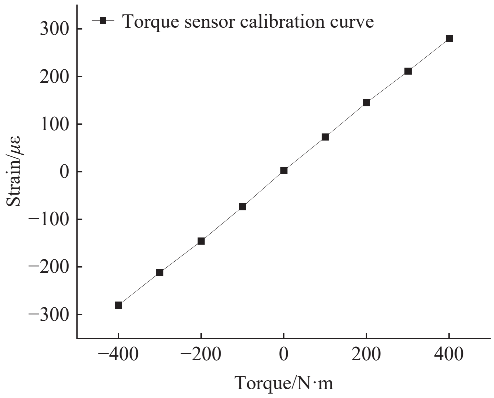

Figure 4 Calibration fitting curve of torque sensor

The damping pad is pasted on the surface of the treated drive shaft and firmly bonded to the contact surface of the shaft by AB glue. The torque acquisition module is installed on the damping pad and fixed at the same time to reduce the interference of the bridge vibration on the acquisition module. After the installation, the signal debugging is carried out in the combine harvester cab using the special test software.

3.2.2 Test system installation

The speed acquisition module, which used Hall sensors, was installed at the connection between the drive components and the shaft via the connection fixture. During installation, the coplanarity of the drive surfaces and the coaxial alignment between the Hall sensor and the drive shaft were ensured. Shims were installed between the sensor and the base to mitigate the effects of bending moments and vibrations on speed measurement.

Each acquisition module was installed as shown in Figure 5. After wiring was completed, the main power supply was turned on, and communication debugging was performed. The main steps were as follows: 1) Network setup; 2) eDAQ signal test software setup; 3) Acquisition channel matching and sampling parameter settings: The sampling frequency was set to 1024 Hz, and the sampling duration was consistent with the actual harvesting operation time of the combine harvester; 4) The experimental prototype was started and the data sampling was carried out.

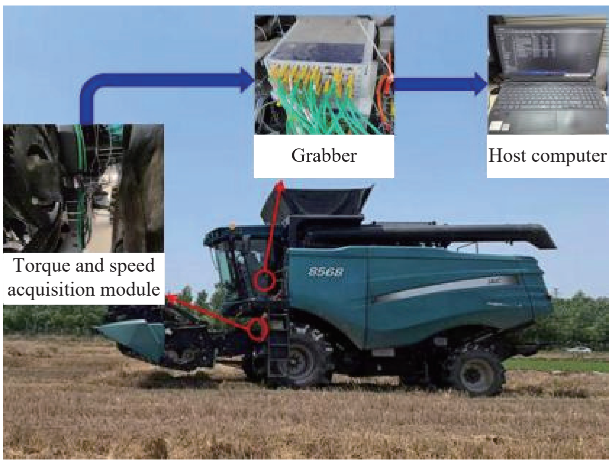

Figure 5 Installation diagram of test system

4 Field load testing and load spectrum

4.1 Test protocol

The test selected a domestic large feed capacity wheeled combine harvester (feed capacity 12 kg/s) as the test subject. Field load tests were conducted during the wheat harvest period in Yanshi District, Luoyang City, Henan Province in June 2024, as shown in Figure 6. The test was carried out under the condition of full header feeding (no partial feeding), constant engine speed (2200 r/min), and the combine harvester moved in a straight line without turning during the data acquisition period to ensure the stability of the operating conditions. The tests were conducted without interfering with the operator's work throughout the process, and the tests were carried out in accordance with local operation characteristics and harvest path habits while meeting the crop harvest conditions and grain loss rate standards[21]. The parameters of the test machine are listed in Table 2, and the test conditions and wheat crop conditions are listed in Table 3.

Figure 6 Field test photograph

Table 2 Performance parameters of test prototypes

Name	Parameters
Overall dimensions/mm	10 150 × 6360 × 3950
Matching engine power/kW	176
Overall mass/kg	14 000
Cut width/mm	5800
Feed volume/kg·s^{-1}	12

Table 3 Test conditions and wheat crop conditions

Name	Parameters
Test ground length×width/m	50×20
Surface conditions	No sunken feet, no standing water, no weeds
Crop varieties	Elymus 307
Maturity	Maturity period
Degree of lodging	No lodging
Grain moisture content/%	12.4
Natural height of the crop/mm	765

The tests selected the torque data from the full width of the combine harvester header feeding (5800 mm), the forward gear D_1 with a large throttle ((6.0±0.5) km/h) entering the stable test area to the end of the harvest as the test data, and took the average of three operations. The corresponding shaft power can be calculated by the torque and speed of the drive shaft, that is

$$T = 9550P/n \tag{2}$$

where, T is the torque value, N·m; P is the power value, kW; n is the speed value of the drive shaft of the feeding and conveying device for combine harvester, r/min.

4.2 Test data processing and load spectrum compilation

4.2.1 Data preprocessing

Due to the harsh conditions, the original data signal is often mixed with abnormal peak points, interfering with data analysis and processing. The nCode GlyphWorks software (GlyphWorks V19.0.0 Release Build 295, HBM United Kingdom) was used to filter and denoise the sampled data by combining amplitude threshold detection, gradient threshold detection, and variance detection to eliminate outliers. Figure 7 shows the torque and power waveforms after preprocessing. Tests showed that the peak power consumption was 4.06 kW and the average power consumption was 1.56 kW under the harvesting operation condition of the drive shaft of the feeding and conveying device for combine harvester.

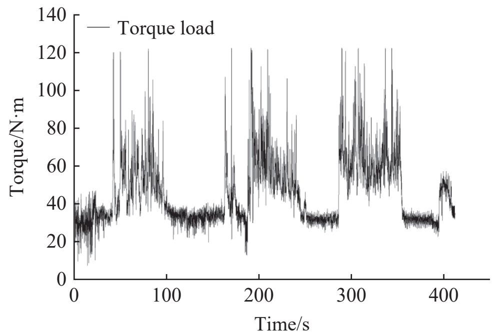

a. Torque waveform diagram

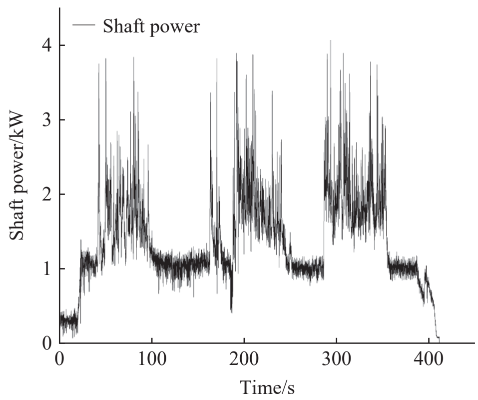

b. Axis power waveform diagram

Figure 7 Preprocessed torque and power waveforms

4.2.2 Load cycle counting

Rainflow counting, which counts the time course of loads, is widely used in fatigue load course analysis[22,23]. By converting the continuous load time course into a series of load cycles and converting the time-domain load data into mean and amplitude load data within the rain basin, the load mean and amplitude frequency relationship was obtained as shown in Figure 8.

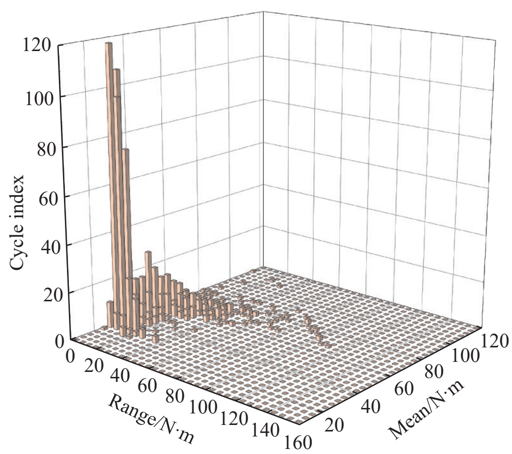

Figure 8 Three-dimensional graph of the joint distribution of average amplitudes

4.2.3 Load independence test

In order to obtain the extrapolation extreme value and extrapolation frequency of the mean and amplitude loads, the independence test of the mean and amplitude loads was carried out based on Fisher's theorem. If the mean and amplitude are independent of each other, the data approximately obey the chi-square distribution with degrees of freedom of $(r-1)(s-1)$[24].

$$\chi^2 = n\sum_{i=1}^{r}\sum_{j=1}^{s}\frac{\left(n_{ij}-\frac{n_i\cdot n_j}{n}\right)^2}{n_i n_j} \tag{3}$$

where, n is the sample length of each operation segment; r and s are the number of grades of amplitude and mean; n_i is the frequency of the amplitude at level i; n_j is the number of times the mean is at level j; n_{ij} is the frequency at which the load cycle falls to the i-th amplitude and the j-th mean.

The mean and amplitude of the torque load on the drive shaft of the feeding and conveying device for combine harvester were divided into 64 levels. The upper percentile point data of the χ^2 distribution at 0.05 was approximately obtained as 1977. Therefore, according to Equation (3), less than 1977 is χ^2 calculated, and it can be assumed that the mean and amplitude of the torque load are independent of each other at a confidence level of 0.95. Therefore, under the condition of mutual independence, the combined distribution function of the mean and amplitude loads is the product of their respective distribution functions.

By conducting the average amplitude probability distribution test on the resulting statistical frequency distribution matrix, it was determined that the load mean obeyed the normal distribution and the load amplitude obeyed the Weibull distribution, which conformed to the characteristics of random stress load data. The joint probability density function is as shown in Equation (4).

$$f(x,y)=\frac{\alpha}{\beta}\left(\frac{x-\varepsilon}{\beta}\right)^{\alpha-1}e^{\left\{\left(\frac{x-\varepsilon}{\beta}\right)^{\alpha}\right\}}\frac{1}{\sqrt{2\pi\delta}}e^{\left\{\frac{(y-\mu)^2}{2\delta^2}\right\}} \tag{4}$$

In the formula, x is the measured load amplitude; y is the average measured load; α is the shape parameter of the Weibull distribution; β is the size parameter of the Weibull distribution; ε is the threshold parameter of the Weibull distribution; μ is the mean of the normal distribution; δ is the standard deviation of the normal distribution.

4.2.4 Two-dimensional extrapolation load spectrum

Considering the test cost, the load spectrum collected by the test is only the load spectrum under typical operating conditions in a short time, which leads to the fact that some of the large loads that should appear in theory do not appear, and these large loads often have a great impact on the fatigue damage of the drive shaft[25,26]. To obtain the possible load history throughout the entire life cycle, the cumulative frequency of loads must be extended to 10^6 times[27]. Based on the fatigue cumulative damage theory and Miner criterion, this extrapolation scale can fully retain the high-frequency and low-amplitude load information that dominates fatigue damage, ensuring the accuracy of fatigue life evaluation for the drive shaft. The extended frequency calculation equation is shown below.

$$N_i' = \frac{10^6}{N}N_i \tag{5}$$

where, N_i' is the cumulative frequency after load expansion in a certain operation section, N is the total cycle frequency of the load, and N_i is the frequency of the tested load.

Since the mean and amplitude of each segment were independent of each other and satisfied the normal distribution and the Weibull distribution respectively, finding the extreme value of the load can be transformed into finding the maximum mean and amplitude[28]. Based on the probability density function of the load and the probability P of the extreme value, the extreme value of the amplitude was calculated according to Equation (6), and the extreme value of the mean value was calculated according to Equation (7).

$$X_{\max} = \varepsilon + \beta^{\alpha\sqrt{-\ln P}} \tag{6}$$

$$Y_{\max} = \mu_p \sigma + \mu \tag{7}$$

where, μ_p is the standard normal deviation.

According to the maximum values of the load mean and amplitude, the mean was classified into 8 levels by equal interval classification method, and the amplitude was classified into 8 levels by unequal interval classification method. The reason for adopting this method was based on the common industry practices and relevant specifications for load spectrum compilation, with the 8-level grading balancing the accuracy of the load spectrum and operability of bench fatigue tests to avoid complicated test procedures from excessive grading and loss of load characteristics from insufficient grading. The number of cycles of the mean and amplitude loads at each level was obtained based on the joint probability density function of the mean and amplitude, and finally the two-dimensional extrapolation load spectrum of a certain operating section under typical conditions of the drive shaft of feeding and conveying device for combine harvester was obtained, as listed in Table 4.

Table 4 Two-dimensional extrapolation load spectrum of a certain working section

Mean/N·m	Range/N·m							
	7.25	21.74	36.24	50.73	65.23	79.72	94.22	108.71
115.22	0	0	0	0	0	0	0	0
100.87	0	0	0	0	0	0	0	0
86.52	82	384	302	0	0	0	0	0
72.17	1034	1343	959	1131	881	398	83	82
57.82	10 000	14 850	6048	1844	1038	398	82	83
43.47	15 160	15 980	1375	554	0	0	0	0
29.11	6499	7116	616	0	0	0	0	0
14.76	389	389	0	0	0	0	0	0

The two-dimensional extrapolated load spectrum can be directly used as the loading basis for the bench fatigue life test of the drive shaft of the feeding and conveying device for combine harvester to guide the structural optimization and anti-fatigue design of the drive shaft; it can also provide a standardized reference scheme for the power matching and load spectrum compilation of conveying components of the same type of agricultural machinery, promoting the engineering improvement of the reliability of agricultural machinery transmission systems.

5 Conclusions

1) Based on the BF350 high-precision full-bridge strain gauge and HT035018-018 shaft end slip ring, a load test system for the drive shaft of the feeding and conveying device for combine harvester was constructed. Load data of the combine harvester under typical operating conditions were obtained. The maximum power was 4.06 kW and the average power was 1.56 kW under harvesting operation conditions.

2) Based on the statistical analysis theory, the two-dimensional extrapolation load spectrum of the drive shaft of the feeding and conveying device for combine harvester under the typical working condition was compiled by using the matrix cycle extrapolation method based on the rainflow counting method, which can provide loading conditions for the fatigue life load test of the drive shaft of the feeding and conveying device for combine harvester.

3) The integrated method of field load test system construction and two-dimensional extrapolation load spectrum compilation based on rainflow counting and matrix cyclic period extrapolation can provide a basis for the power matching of the combine harvester working device's drive shaft, and provide a technical reference for the anti-fatigue design of the combine harvester transmission system.

Acknowledgements

The authors acknowledge that this work was supported by the National Natural Science Foundation of China (Grant No. 52075149), Henan Province key research and development project (Grant No. 251111110800), Frontier Exploration Projects of Longmen Laboratory (Grant No. LMQYTSKT032), Graduate Education Reform Project of Henan Province (Grant No. 2023SJGLX180Y), and Postgraduate Education Reform and Quality Improvement Project of Henan Province (YJS2025AL49).

[References]

[1] Liu F. Maintenance and troubleshooting of wheat combine harvester. Xinjiang Agricultural Mechanization, 2024; 6: 58–60. (in Chinese)
[2] Zhao Z Y. Feeder of combine structure optimization research. MS dissertation, Harbin: Northeast Agricultural University, 2019. (in Chinese)
[3] Jin F, Yang S H, Zhang J S, Li Q X, Che K, Pang T. Design and experiment of variable gap conveying device for corn kernel harvester. Transactions of the CSAM, 2025; 56(7): 349–360. (in Chinese)
[4] Wang G Q, Li Y M, Wang R, Wang L, You X Q, Huang B B. Dynamic load distribution property of transmission system during rice harvesting process. Advances in Mechanical Engineering (Sage Publications Inc.), 2024; 16(1): 1–16.
[5] Yang Z H, Huang S C, Zhu H Y, Chen D, Zhu Z X, Song Z H. Accelerated editing for the load spectrum of harvester operational units using optimal wavelet components. Transactions of the CSAE, 2025; 41(2): 58–65. (in Chinese)
[6] Ren C S, Hu J P, Liu W, Zeng T Y, Tan R J. Construction and performance testing of a half axis load testing system for tracked vegetable transplanters. Journal of Agricultural Mechanization Research, 2025; 47(8): 183–189. (in Chinese)
[7] Li G P, Li Y M, Xia S B, Du T, Wu Y. Construction and analysis of load testing system for large feed rate tracked combine harvester. Journal of Agricultural Mechanization Research, 2025; 47(4): 65–69, 76. (in Chinese)
[8] Zhang Q, Wan J Y, Xiong Y Z. Research on load spectrum of fatigue test program for transmission system of construction machinery. Construction Machinery and Equipment, 2021; 52(1): 16–22, 7. (in Chinese)
[9] Liu Y F, Yang J. Research on loader hydraulic torque converter output shaft power test system. Machinery Design & Manufacture, 2022; 8: 108–112. (in Chinese)
[10] Xing W T, Dai Y F, Zhu C, Lan Q H, Ye X M, Cheng X B. Experimental research on shafting strain testing system. Electronic Test, 2021; 13: 12–15. (in Chinese)
[11] Li J, Han C Y, Wu W B, Tang T, Ran X, Zheng Z F, et al. Load spectrum compilation method of hybrid electric vehicle reducers based on multi-criteria decision making. Energies, 2022; 15(9): 3293.
[12] Chin C, Abdullah S, Yin A, Ariffin A. Vibration fatigue analysis through frequency response function of variable amplitude loading. Journal of Mechanical Science and Technology, 2022; 36: 33–43.
[13] Manouchehrynia R, Abdullah S, Singh S S K, Correia J. Reliability-based fatigue life assessment using random road load condition and local damage criteria. Engineering Failure Analysis, 2023; 146: 107157.
[14] Wang Y H, Li H Z, Song L X. Compilation of load spectra for hydraulic shock absorbers of electric bicycles based on rainflow counting method. Construction Machinery and Equipment, 2025; 56(9): 17–21. (in Chinese)
[15] Xiao X T. Research on the method of compiling load spectrum of tractor transmission shaft. MS dissertation. Yangling: Northwest Agriculture & Forestry University, 2025; p. (in Chinese)
[16] Xiong G L, Li Y, Deng Y, Huang D, Wu X, Zhu C C. High-cycling fatigue life assessment of vehicle hypoid gears based on load spectrum. Journal of

Mechanical Strength, 2025; 47(2): 61–67. (in Chinese)
[17] Chen Y Z, He Y J. Compilation and application of load spectrum for planar mobile three-dimensional garage transportation system. Progress in Steel Building Structures, 2025; 27(6): 95–103. (in Chinese)
[18] Xuan M H. Research on assembly quality inspection of inclined conveyor device of combine harvester. MS dissertation. Luoyang: Henan University of Science and Technology, 2022; 51p. (in Chinese) doi: 10.27115/d.cnki.glygc.2022.000731
[19] Li S. Design and experiment on key components of the intermediate conveying device of oil sunflower combine harvester. MS dissertation. Wuhan: Huazhong Agricultural University, 2020; 55p. (in Chinese) doi: 10.27158/d.cnki.ghznu.2020.000246
[20] Arai K, Shimazu M, Umeda N, Kurihara E. Study of grain conveyor structure to reduce cleaning time of combine harvester. Japan Agricultural Research Quarterly: JARQ, 2019; 53(4): 247–253.
[21] The work quality of corn (wheat) combine harvester. NY/T 995-2006, 2006. (in Chinese)
[22] Huang P, Lu J S, Ding H F, Chen Z M, Zhao Y Q. Fatigue life prediction of a new loader working device. Journal of Mechanical Engineering, 2025; 61(17): 27–40. (in Chinese)
[23] Wei Y C, Yuan X L, Zhao X, Chen X Y, Du J Y. Compiling load spectra for electric vehicle drive systems with strong user association. Chinese Journal of Automotive Engineering, 2025; 15(4): 590–602. (in Chinese)
[24] Zhai X T, Chen M D. Load spectrum compiling of peanut combine harvester's seedling clamping and conveying system. Transactions of the CSAM, 2020; 54(S1): 261–266, 363. (in Chinese)
[25] Liu P, Li H Y, Zhao B Y, Tian H L, Wang X, Zhou L M, et al. Research on vehicle torque spectrum compilation based on real-vehicle operation data acquisition device development and Goodman rainflow cycle counting method. China Auto, 2024; 8: 36–42. (in Chinese)
[26] Zhang C F. Research of load spectrum acquisition and durability of drive shaft system. MS dissertation. Guangzhou: South China University of Technology, 2023; 67p. (in Chinese) doi: 10.27151/d.cnki.ghnlu.2023.001274
[27] Zhai X T, Zhang X C, Jiang Z J, Li Y Y, Zhang Q, Wang J X. Load spectrum compiling for wheel loader semi-axle based on mixed distribution. Transactions of the CSAE, 2018; 34(8): 78–84. (in Chinese)
[28] Zhang Y S, Wang G Q, Wang J X, Jia H B, Zhang E P. Compilation method of power train load spectrum of engineering vehicle. Transactions of the CSAE, 2011; 27(4): 179–183. (in Chinese)